TIRAP p.R81C is a novel lymphoma risk variant which enhances cell proliferation *via* NF-κB mediated signaling in B-cells

Regula Burkhard,[1,2,3] Irene Keller,[4] Miroslav Arambasic,[1,2,3] Darius Juskevicius,[5] Alexandar Tzankov,[5] Pontus Lundberg,[6] Rémy Bruggmann,[4] Stephan Dirnhofer,[5] Ramin Radpour[1,7]* and Urban Novak[1,3]*

[1]Department of Medical Oncology, Inselspital, Bern University Hospital; [2]Division of Experimental Pathology, Institute of Pathology, University of Bern; [3]Department for BioMedical Research (DBMR), University of Bern; [4]Interfaculty Bioinformatics Unit, Department for Bio-Medical Research, and Swiss Institute of Bioinformatics, University of Bern; [5]Institute of Pathology and Medical Genetics, University of Basel; [6]Department of Biomedicine, Experimental Hematology, University Hospital Basel and University of Basel and [7]Tumor Immunology, Department for BioMedical Research (DBMR), University of Bern, Switzerland

RR and UN are co-senior authors.

Correspondence: *URBAN NOVAK*

urban.novak@insel.ch

Supplemental methods, tables and figures

TIRAP p.R81C is a novel lymphoma risk variant which enhances cell proliferation via NF-κB mediated signaling in B-cells

Regula Burkhard[1,2,3], Irene Keller[4], Miroslav Arambasic[1,2,3], Darius Juskevicius[5], Alexandar Tzankov[5], Pontus Lundberg[6], Rémy Bruggmann[4], Stephan Dirnhofer[5], Ramin Radpour[1,7,*] and Urban Novak[1,3,*,+]

[1] Department of Medical Oncology, Inselspital, Bern University Hospital, University of Bern, Bern, Switzerland.

[2] Division of Experimental Pathology, Institute of Pathology, University of Bern, Bern, Switzerland.

[3] Department for BioMedical Research (DBMR), University of Bern, Bern, Switzerland.

[4] Interfaculty Bioinformatics Unit, Department for BioMedical Research, and Swiss Institute of Bioinformatics, Bern, Switzerland.

[5] Institute of Pathology and Medical Genetics, University of Basel, Basel, Switzerland.

[6] Department of Biomedicine, Experimental Hematology, University Hospital Basel and University of Basel, Basel, Switzerland.

[7] Tumor Immunology, Department for BioMedical Research (DBMR), University of Bern, Bern, Switzerland.

[*] Co-senior authors

[+] to whom correspondence should be addressed

Supplemental methods

Analysis of somatic variants

Somatic variant calling and annotation. For the identification of somatic variants, the reads produced from germline and tumor samples of both sisters were mapped to the human reference genome (hg19) using bwa-mem v.0.7.5a, and PCR duplicates were identified with Picard-tools v.1.8.[1] Somatic variants were called using Strelka v.1.0.10 and SomaticSniper v.1.0.4.[2,3] Strelka was run using the configuration file for bwa provided with the tool, with default values for all options except isSkipDepthFilters which was set to 1 as recommended for WES data. Post-call filtering was applied as previously outlined.[2] In the SomaticSniper analysis, reads with a mapping quality of 0 were ignored and default values were used for all other options. Quality filtering was performed using our own script to retain only variants with at least three reads per allele and strand, and minimum base and mapping qualities of 30 for each allele. The variants detected by Strelka or SomaticSniper were combined and annotated using SnpEff v.3.2. in cancer mode.

Verification of somatic variants by Ion-Proton sequencing. To confirm somatic mutations identified by WES using the Illumina technology, we resequenced the tumor DNA from both sisters on an Ion-Proton sequencing system (Thermo Fisher Scientific). Library preparation was performed using the IonXpress Plus Fragment Library Kit (Thermo Fisher Scientific) according to the manufacturer's protocol. The resulting DNA libraries were pooled for the subsequent exome capturing which was performed with the Ion Target Exome Kit (Thermo Fisher Scientific). The enriched DNA libraries were then sequenced in a 500 flows run on a Proton instrument using V3 chemistry. The library preparation and sequencing was performed by Fasteris.

CLC Genomics Workbench software v.7.5.1 (Qiagen) was used to map the reads against the human reference genome (hg19) and perform a local realignment around indels. Variants were called using the Low Frequency Variant Detection tool, using a minimum coverage of 8, a minimum count of 2 and a minimum frequency of 20%.

Additionally, we compiled the total number of Ion Proton reads supporting each base at all positions where somatic variants had been detected based on the Illumina data. The goal of this step was to obtain tentative confirmation of variants at positions with low sequencing depth in the Ion Proton data. The base counts were compiled using the GATK's DepthOfCoverage tool based on alignment files produced with the Ion Reporter software by Fasteris.

Sanger Sequencing and validation of TIRAP p.R81C variant

TIRAP p.R81C variant and the expression of the mutated allele were assessed by sanger sequencing of cDNA isolated from peripheral blood mononuclear cells (PBMCs) of all family members. Primer sequences for validation are listed in Supplemental Table 6.

Isolation and in vitro culture of PBMCs

PBMCs from healthy donors or members of the studied family were isolated by density gradient centrifugation using Lymphoprep (Axis-Shield). Isolated cells were cultured in RPMI-1640, supplemented with 50 U/ml penicillin, 50µg/ml streptomycin (Sigma Aldrich) and 10% heat-inactivated human AB serum (Swiss Red Cross).

Proliferation assay and flow cytometry

PBMCs were cultured overnight in the presence or absence of 10ng/ml LPS (Thermo Fisher Scientific). Cells were stained with anti-CD20-PerCp-Cy5.5 (Biolegend). Intracellular staining with anit-Ki-67-PE (BD Bioscience) was performed using the Foxp3 staining Buffer set (eBioscience). After the final washing step, cells were resuspended in staining Buffer containing DAPI and incubated for 30 min. For live/dead cell discrimination, cells were washed in annexin V binding buffer (BD Bioscience) and stained with annexin V-FITC and DAPI (both Biolegend). Flow cytometry was performed using an LSR II (BD Biosciences) and analyzed with FlowJo software v.10 (TreeStar). Antibodies applied in this study are listed in Supplemental Table 4.

Small interfering RNA (siRNA)-mediated silencing of TIRAP gene

PBMCs were transfected with 50nM of commercially available human *TIRAP* (sc-42932) or scrambled siRNA (sc-37007, both Santa Cruz Biotechnology) using Lipofectamine LTX (Thermo Fisher Scientific) according to manufacturer's protocol and incubated for 16 hours in the presence or absence of 10ng/ml LPS. Thereafter, cells were subjected for the targeted gene expression or flow cytometry analysis.

Functional analysis of TIRAP p.R81C variant

Total of $8x10^5$ HEK 293T cells were seeded in 6-well plates and transiently transfected with 500ng of GFP-expressing constructs (pCCL.sin.PPT.hPGK.GFPWpre backbone) encoding TIRAP wild-type, TIRAP p.R81C or empty vector control. Twenty-four hours post transfection, cell viability and apoptosis were measured on GFP-positive cells. Therefore, cells were washed in Annexin V binding buffer (BD Bioscience) and stained with Viability Dye eFluor® 450 (eBioscience) and PE Annexin V (Immunotools). FACS-sorting was performed using FACS ARIA. Sorted GFP-positive cells were either used for RNA extraction (see below); or seeded at equal numbers in starvation medium (EBSS (Sigma) supplemented with 1% FCS) and incubated for 24 or 48 hours.

Targeted gene expression analysis

RNA from PBMCs of all family members or from transfected 293T cell was purified using RNeasy micro kit (Qiagen) and transcribed into cDNA using the High-Capacity cDNA Reverse Transcription kit (Thermo Fisher Scientific). In all PBMC samples, the total lymphocyte population accounted for 65% on average based on forward and site scatter in flow cytometry. qRT-PCR was assessed for a panel of selected genes (Supplemental Table 6) using FastStart Universal SYBR Probe Master (Roche). All reactions were performed on an ABI 7500 (Applied Biosystems) platform. Expression

levels of genes were normalized to *ACTb* mRNA and cells treated with *TIRAP* siRNA versus scrambled (CTRL) siRNA were compared using the $2^{-\Delta\Delta CT}$ method. Gene expression data was clustered using standard Euclidean's method based on the average linkage. Heatmaps were generated according to the standard normal distribution of the values (standardize makes mean of each column as zero, and scale it to standard deviation of 1 to making all the columns equal weight).

Array comparative genomic hybridization

For each hybridization, at least 300ng of genomic DNA from each sample and 500ng of commercial sex-matched 46 XX reference genomic DNA (Promega) were used. Reference and normal genomic DNA of sister 1 and 2 were digested by heat fragmentation at 95°C for 35 minutes. FFPE tissue-derived tumor samples needed no additional digestion. DNA fragmentation was evaluated by gel electrophoresis and image analysis with the ImageJ software (NIH). Subsequent sample labelling, hybridization and data analysis was performed as described.[4]

Immunohistochemistry

Immunohistochemistry was performed on serial tissue sections either manually overnight at 4°C or using an automated immunostainer Benchmark XT (Ventana/Roche) with a biotin-streptavidin peroxidase detection system according to the manufacturer's recommendations. For antibodies applied, see Supplemental Table 4. Cell of origin classification was done based on immunohistochemistry, as suggested by the current WHO classification[5], applying the so-called Tally algorithm, which has been proven to give the best concordance with microarray data.[6]

Fluorescent in situ Hybridization

Fluorescence *in situ* hybridization (FISH) was performed according to standard protocols on paraffin sections using bacterial artificial chromosome (BAC) clones for the 5' and 3' region of *JAK2* gene, BAC probes spanning the *TNFAIP3* gene in combination with a centromeric probe for chromosome 6 as described previously.[7,8] A Break Apart FISH assay designed to identify rearrangements of *CIITA* (16p13.13) was performed with a telomeric and centromeric BAC probe. Chromosomal translocations affecting *MYC* and *BCL2* were assessed by FISH using commercially available break apart probes from Vysis (Abott Molecular).[9] For further information see Supplemental Table 5.

Validation of GSTT1 loss

GSTT1 deletion status was examined by multiplex PCR in the tumor and matched normal DNA of both siblings as well as the germline DNA of healthy family members. Primer sequences for validation are listed in Supplemental Table 6.

Statistical analyses

Statistical analyses were performed using GraphPad Prism v.7 (GraphPad Software). Results are expressed as mean ± SEM if not stated otherwise. Comparisons were drawn using unpaired t-test,

Mann–Whitney U test or one-way Annova with Bonferroni post hoc test. The p values <0.05 were regarded as statistically significant with *p<0.05*, **p<0.01*, and ***p<0.001* (95% confidence interval).

Supplemental table 1. Characteristics of the lymphomas, treatment and outcome.

Patient	Age at diagnosis	Staging / involved sites	Diagnosis	Treatment	Outcome
Sister 1	30 years	IAE (mediastinal bulk)	PMBL	6x R-CHOP, 1x R, salvage with high-dose MTX & cytarabine and R-ICE	Died with primary progressive disease
Sister 2	25 years	II A / anterior mediastinum, supraclavicular region	Non-GC DLBCL NOS with features of PMBL	6x R-CHOP	Ongoing remission

Abbreviations: DLBCL, diffuse large B-cell lymphoma; GC, germinal center; NOS, not otherwise specified; r, rituximab; CHOP, cyclophosphamide, doxorubicin, vincristine, prednisone; ICE, ifosfamide, carboplatin, etoposide; MTX, methotrexate; PMBL, primary mediastinal B-cell lymphoma.

Supplemental table 2. The immunopathological features of the lymphomas.

	Sister 1	Sister 2
Diagnosis	PMBL	Non-GC DLBCL with features of PMBL
EBV	-	-
BCL2	+	-
BCL6	7-8%	1-2%
CD10	+	-
GCET1	+	-
LMO2	80%	20%
FOXP1	7-8%	-
MUM1p	40%	40%
CD20	+	+
CD23	+	-
CD30	+	+
Ki-67	65%	50%
pJAK2	>80%	>80%
pSTAT3	40%	60%
pSTAT6	30%	50%
TNFAIP3 FISH	2n	2n
BCL2 FISH	2n / no break	2n / no break
MYC FISH	5n	2n
CIITA FISH	Break apart	No break
JAK2 FISH	9p24 (gain)	9p24 (gain)

Abbreviations: DLBCL, diffuse large B-cell lymphoma; GC, germinal center; -, negative staining, +, positive staining.

Supplemental table 3. Exome data metrics.

Sample	Enrichment kit	Sequenced in (year)	Read pairs (mio)	Bases (GB)	mapped unique reads (#)	Mean coverage ±100bp (fold)
Sister 1 Tumor	TrueSeq (15013230 Rev. A)	2012	32	6.39	13.5 mio 46.2%	20
Sister 1 Germline	TrueSeq (15013230 Rev. A)	2012	63	12.62	43.5 mio 70.6%	61
Sister 2 Tumor	TrueSeq (15013230 Rev. A)	2012	48	9.68	3.1 mio 6.9%	4
Sister 2 Germline	TrueSeq (15013230 Rev. A)	2012	55	11.01	39.6 mio 74.0%	55.9
Sister 2 Tumor	Nextera (15032301 Rev. A)	2013	96	26.2	19.8 mio 23.1%	12.1
Sister 2 Germline	Nextera (15032301 Rev. A)	2013	54	9.7	33.2 mio 75%	32.6
Mother Germline	TrueSeq (15013230 Rev. A)	2013	53	10.63	48.3 mio 95.3%	53.82
Father Germline	TrueSeq (15013230 Rev. A)	2013	52	10.42	48 mio 95.1%	56.41
Brother Germline	TrueSeq (15013230 Rev. A)	2014	45	8.9	29.1 mio 74 %	28.9

Supplemental table 4. Antibodies used for Flowcytometry (FC) and immunohistochemistry (IHC) on formalin-fixed paraffin-embedded tissue, antigen retrieval procedure and cut-off scores for IHC.

Antibody	Appli-cation	Clone	Conjugated to	Catalog #	Source	Cut-off score
BCL2	IHC	SP66	unconjugated	790-4604	Vetana/Roche	70%[10]
BCL6	IHC	GI191E/A8	unconjugated	760-4241	Vetana/Roche	30%[11]
CD10	IHC	SP67	unconjugated	790-4506	Vetana/Roche	20%[11]
CD20	IHC	L26	unconjugated	760-2531	Vetana/Roche	no cut-off
CD23	IHC	SP23	unconjugated	790-4408	Vetana/Roche	any expres-sion
CD30	IHC	Ber-H2	unconjugated	790-4858	Vetana/Roche	any expres-sion
FOXP1	IHC	SP133	unconjugated	760-4611	Vetana/Roche	50%[12]
pIRAK1	IHC	polyclonal	unconjugated	Ab63484	Abcam	15%
IRAK4	IHC	Y279	unconjugated	Ab32511	Abcam	any expres-sion
GCET	IHC	RAM341	unconjugated	Ab68889	Abcam	60%[11]
KI67	IHC	MIB-1	unconjugated	IR626	Dako	no cut-off
LMO2	IHC	1A9-1	unconjugated	790-4368	Vetana/Roche	30%[11]
MUM1p	IHC	MRQ-43	unconjugated	760-4529	Vetana/Roche	70%[11]
PDL1	IHC	E1L3N	unconjugated	13684	Cell signaling	any expres-sion
pJAK2	IHC	C80C3	unconjugated	3776	Cell signaling	>8%[9]
pSTAT3	IHC	D3A7	unconjugated	9145	Cell Signaling	17%[9]
pSTAT5	IHC	C11C5	unconjugated	9359	Cell signaling	16%[9]
pSTAT6	IHC	-	unconjugated	ab28829	Abcam	>5%
CD20	FC	2H7	PerCP/Cy5.5	302326	Biolegend	-
Ki-67	FC	B56	PE	556027	BD	-
AnnexinV	FC		FITC	556419	BD	-
DAPI	FC			422801	Biolegend	-
AnnexinV	FC		PE	31490014	Immunotools	
Live/Dead	FC		PacificBlue	65-0863-14	eBioscience	

Supplemental table 5. Probes for fluorescence *in situ* hybridization (FISH).

Locus	BAC clones	Reference
TNFAIP3	RP11-703G8, RP11-102P5	8
BCL2 Break apart	07J75-001 (Vysis, Abott)	9
cMYC Break apart	05J75-00, 05J91-001 (Vysis, Abott)	9
JAK2 Break apart	RP11-3H3, RP11-2302 and RP11-28A9, RP11-60G18	7
CIITA Break apart	RP11-109M19, RP11-66H6	13

Supplemental table 6. Used primers.

Primer Name	Sequence (5' to 3')
Primers for validation by Sanger sequencing	
GSTT1 Forward	TTCCTTACTGGTCCTCACATCT
GSTT1 Reverse	GCAGCATAAGCAGGACTTCAG
B-Globin Forward	CAACTTCATCCACGTTCACC
B-Globin Reverse	GAAGAGCCAAGGACAGTTAC
TIRAP Forward	GCTGAAGAAGCCCAAGAAGAG
TIRAP Reverse	GCTGCCTTCCAAGTAGGAGAC
Primers for quantitative PCR	
ACTB Forward	GCACCACACCTTCTACAATGAG
ACTB Reverse	GGTCTCAAACATGATCTGGGTC
BIRC5 Forward	CGCATCTCTACATTCAAGAACTG
BIRC5 Reverse	CCAAGTCTGGCTCGTTCTC
BCL2L1 Forward	AGGCGGATTTGAATCTCTTTCTC
BCL2L1 Reverse	AAACACCTGCTCACTCACTG
CDKN2A Forward	CACCAGAGGCAGTAACCA
CDKN2A Reverse	CTGATGATCTAAGTTTCCCGAG
CASP9 Forward	CAGATTTGGCTTACATCCTGAG
CASP9 Reverse	CCGCAACTTCTCACAGTC
IL6 Forward	GTGTGAAAGCAGCAAAGAGG
IL6 Reverse	GGCAAGTCTCCTCATTGAATCC
MYC Forward	TCCTCGGATTCTCTGCTCTC
MYC Reverse	CTTGTTCCTCCTCAGAGTCG
NFKB1 Forward	AAGCACGAATGACAGAGGC
NFKB1 Reverse	TTTCCCGATCTCCCAGCT
TIRAP Forward	GTCACTACGGCCTTACATAGGA
TIRAP Reverse	TCATGGAGCAGCCATCAG

Supplemental Table 7. Confirmed somatic mutations (Included in a separated Excel file).

Excel spreadsheet showing confirmed protein-altering somatic mutations identified in the lymphoma of sister 1 and 2.

Supplemental figure 1. (A) Prediction of potential links between genes with germline variants and terms related to cancer and malignant lymphomas. Genes with variants predicted to be likely pathogenic by five different algorithms are highlighted in red. (B) Gene ontology enrichment analysis of the genes with deleterious variants. Enrichment score >3 are significant, $p<0.05$.
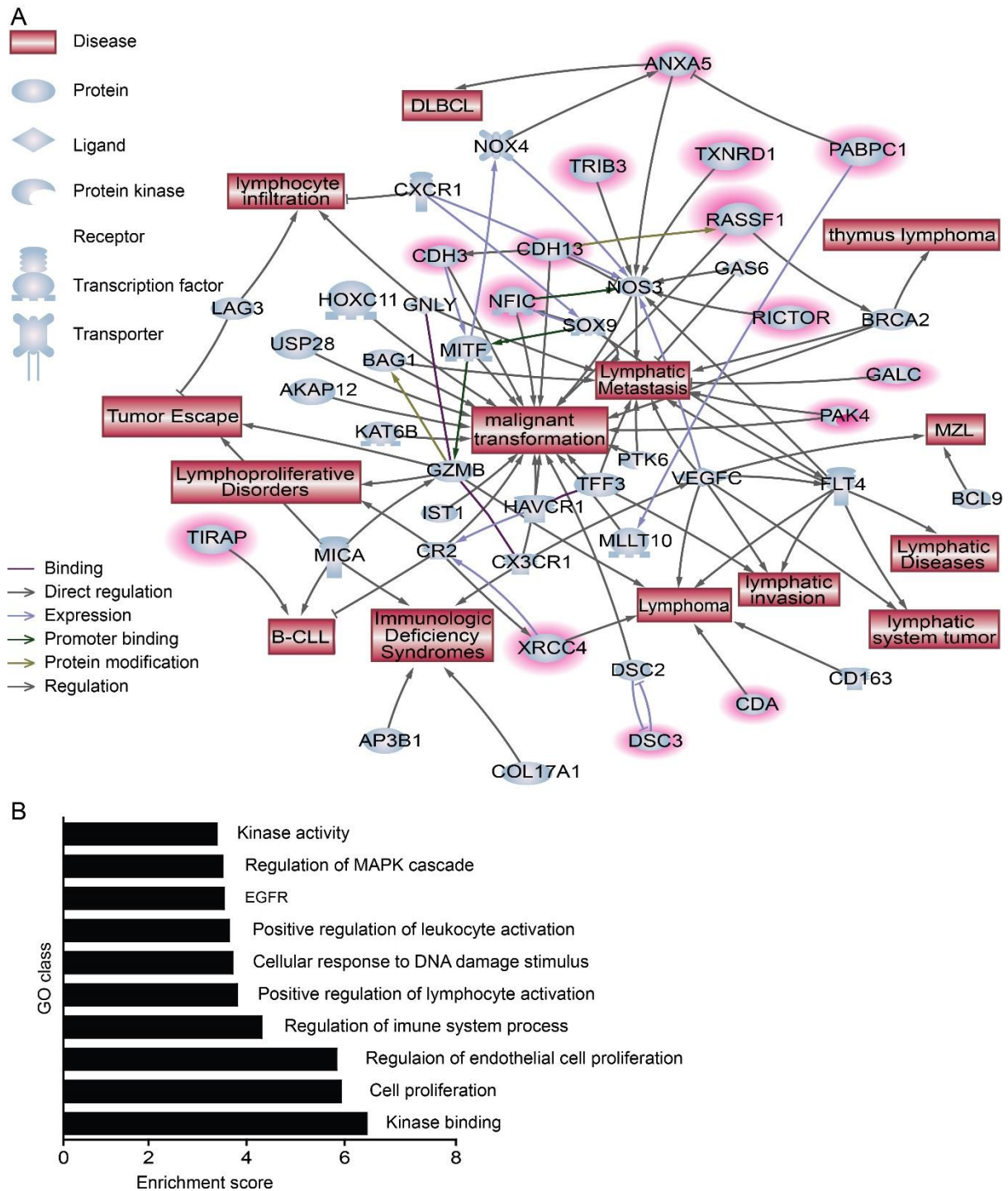
Supplemental figure 2
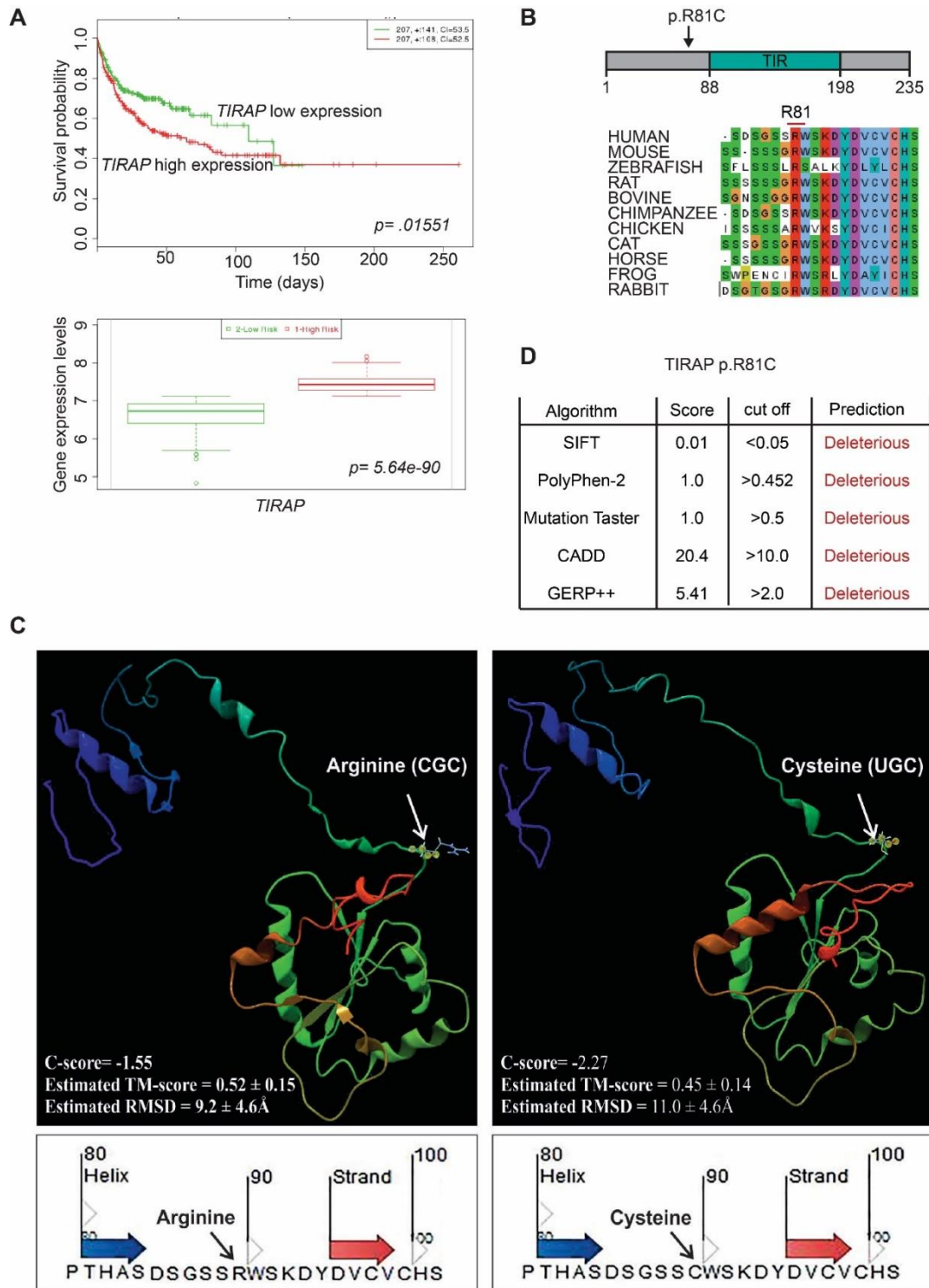
Supplemental figure 2. (A) Analysis of survival and *TIRAP* gene expression in patients with DLBCL. Kaplan-Meier survival curves (top) and box plots (bottom) showing the TIRAP mRNA expression (generated by the SurvExpress program from samples of the GSE10846 dataset). (B) Top: Schematic diagram of the TIRAP protein showing the TIR domain and the position of p.R81C missense mutation. Protein domain annotation according to Pfam. Below: TIRAP amino acid conservation among different species, R81 residue is marked in red. Sequence were aligned using ClustalW2. (C) 3D-structure prediction for TIRAP protein. I-TASSER server was used to generate a full-length model of TIRAP WT (left panel) and TIRAP p.R81C (right panel) by continuous frag-

ments from threading alignments and reassembling them using replica-exchanged Monte Carlo simulations. C-score is a confidence score for estimating the quality of predicted models based on the significance of threading template alignments and the convergence parameters of the structure assembly simulations. TM-score and RMSD are standards to measure the accuracy of structure modeling particularly when the native structure is not known. (D) The effect of the TIRAP p.R81C mutation was assessed in silico by SIFT, PolyPhen-2, MutationTaster, CADD and GERP++.

Supplemental figure 3. Analysis of *TIRAP* p.R81C mutation status by Sanger sequencing of (A) Sequencing result of isolated cDNA from PBMCs of all family members. (B) Genomic DNA isolated from PBMCs of age- and sex-matched healthy donors (HD).
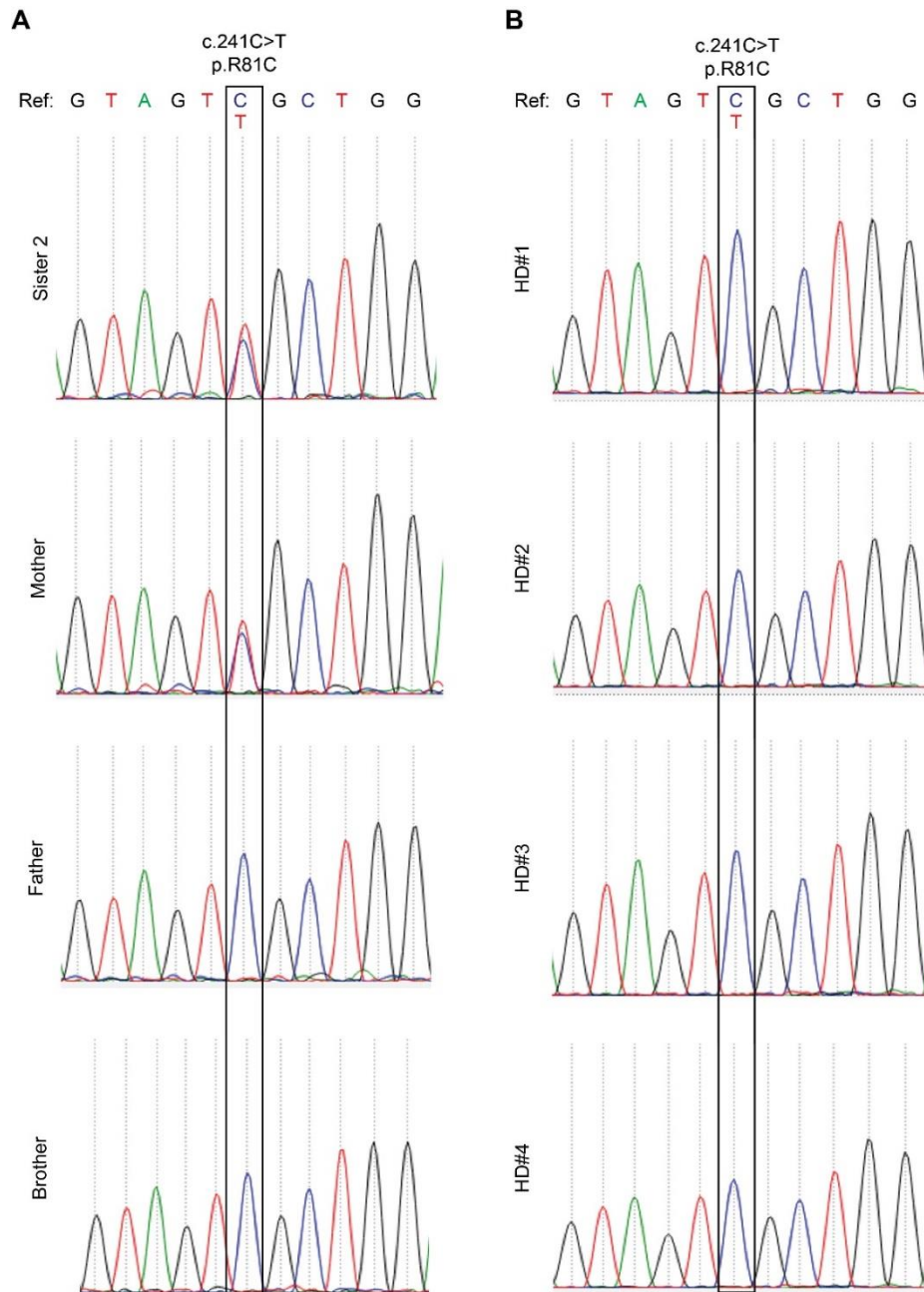
Supplemental figure 4
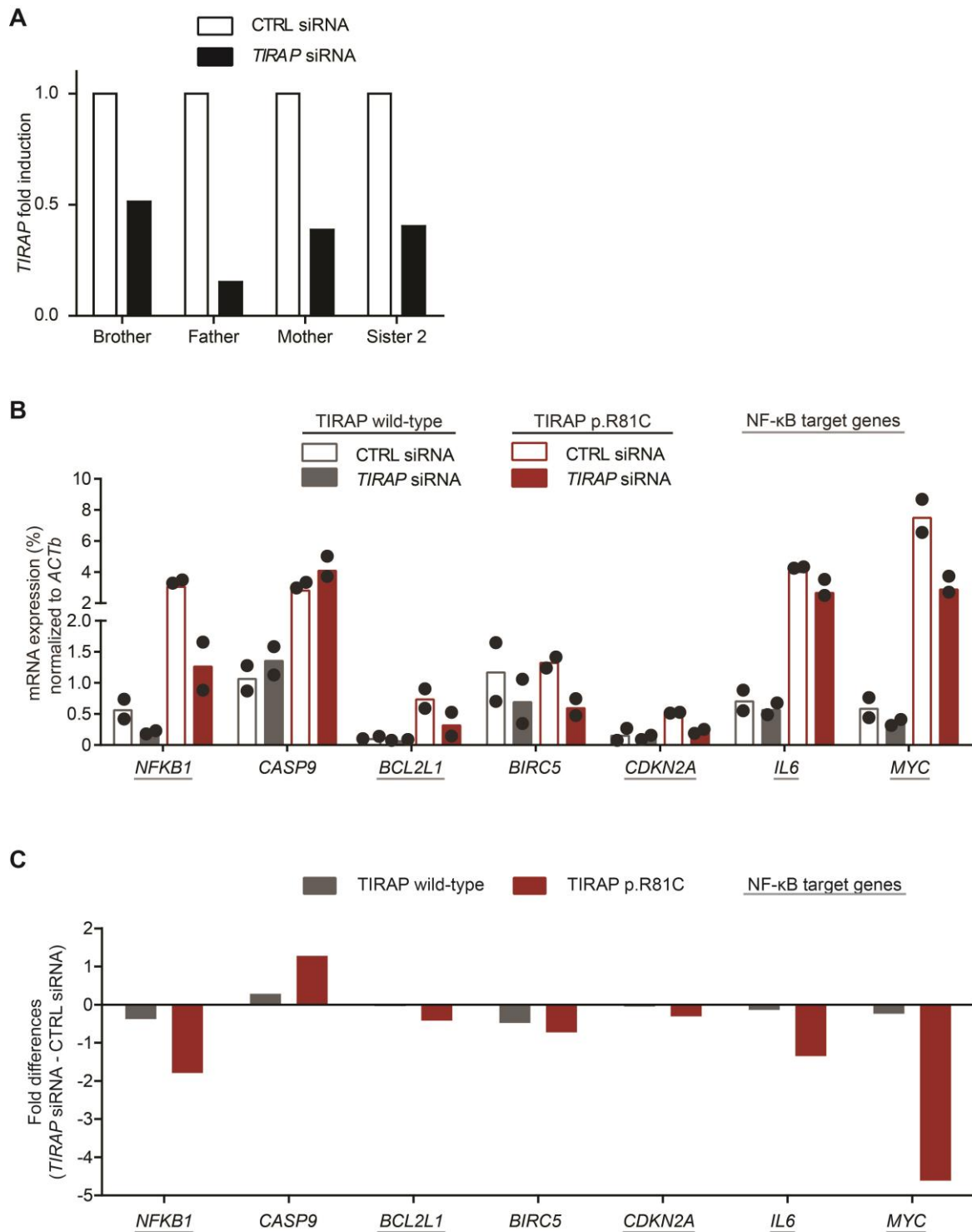
Supplemental figure 4. PBMCs were isolated from family members and transfected with control (CTRL) or *TIRAP*-directed siRNA. (A) Validation of *TIRAP* knockdown efficiency by qRT-PCR 24h post transfection. Values are shown as fold difference compared to cells transfected with CTRL-siRNA. (B) Bar chart showing the relative expression levels of genes involved in NF-κB pathway, cell survival and proliferation normalized to *ACTb* in PBMCs of family members with wild-type (brother and father) and p.R81C (sister 2 and mother) TIRAP. Dots represent values of each individual of the investigated family. (C) The difference of gene expression in cells transfected with *TIRAP* or CTRL siRNA was calculated from mean values shown in panel B.

Supplemental figure 5
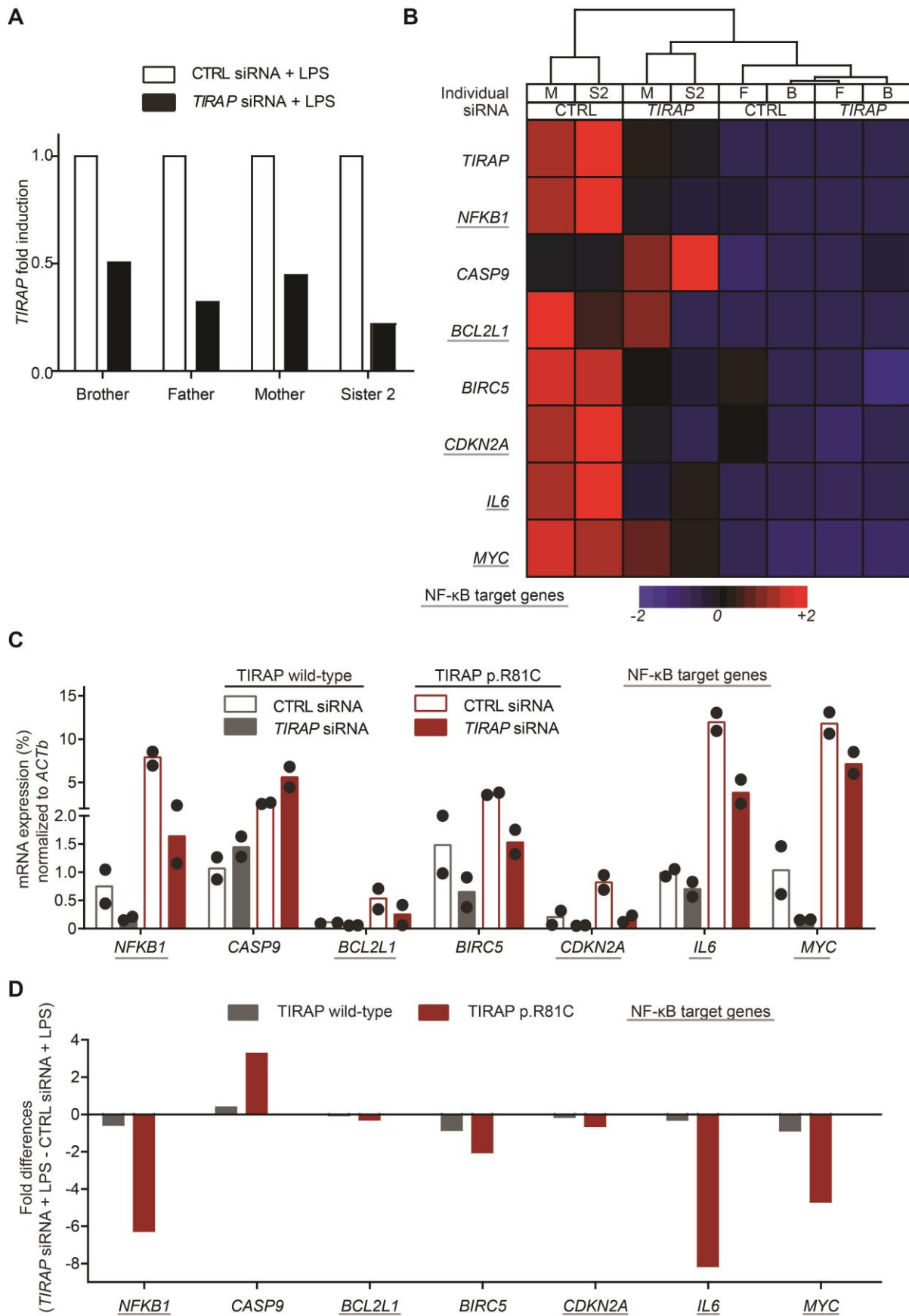
Supplemental figure 5. PBMCs were isolated from family members and transfected with control (CTRL) or *TIRAP*-directed siRNA and cultured in the presence of 10ng/ml LPS. (A) Validation of *TIRAP* knockdown efficiency by qRT-PCR 24h post transfection. Values are shown as fold difference compared to cells transfected with CTRL-siRNA. (B) Heatmap showing hierarchical clustering of eight selected genes involved in NF-κB signaling pathway, cell survival and proliferation in PBMCs of mother (M), sister 2 (S2), brother (B) and father (F) transfected with control (CTRL) or *TIRAP*-directed siRNA and treated with LPS. (C) Bar chart showing the relative expression levels normalized to *ACTb* in PBMCs of family members with wild-type (brother and father) and p.R81C (sister 2 and mother) TIRAP. Dots represent values of each individual of the investigated family. (D) The difference of gene expression in cells transfected with *TIRAP* or CTRL siRNA and treated with LPS was calculated from mean values shown in panel C.

Supplemental figure 6
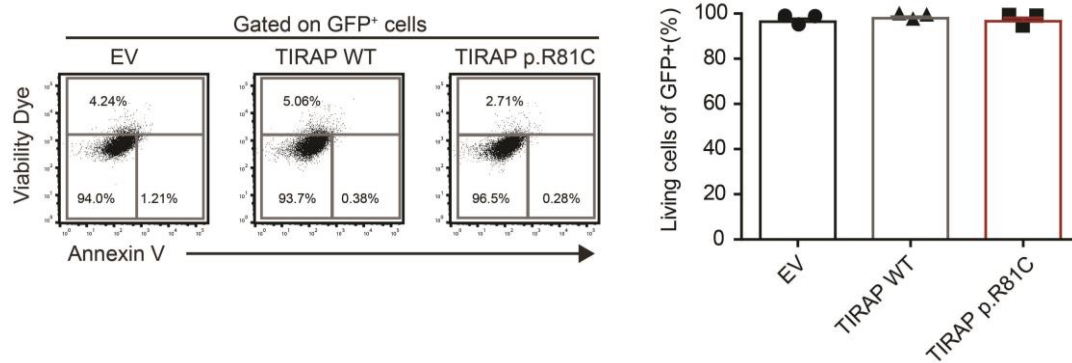
Supplemental figure 6. 293T cells were transiently transfected with TIRAP WT-GFP, TIRAP p.R81C-GFP expressing plasmids or empty vector (EV)-GFP plasmids. Cell viability on GFP-positive cells was assessed 24h post transfection by flow cytometry. Bar chart (mean ± SEM) show percentage of viable cells (AnnexinV- and Viability dye-) of GFP+ cells of three independent experiments.

Supplemental figure 7
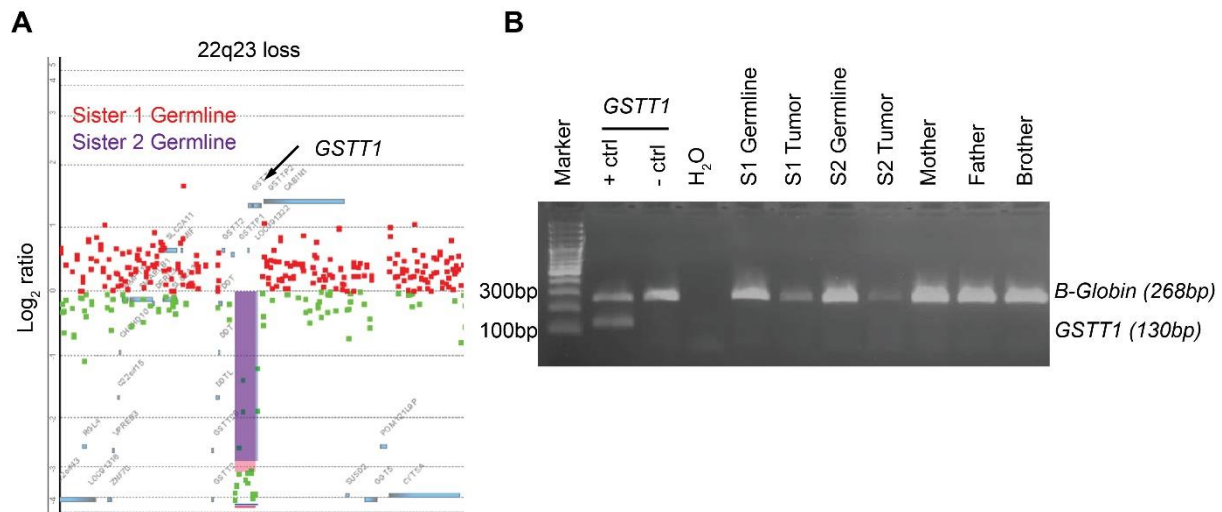
Supplemental figure 7. (A) aCGH probe view of the 22q loss in sister 1 (red) and 2 (purple). The *GSTT1* locus is indicated by an arrow. (B) *GSTT1* gene loss was analyzed in genomic DNA of all family members by a multiplex PCR using *B-globin* as an internal control. The resulting PCR products were analyzed on a 1.5% agarose gel. Amplification of *GSTT1* yields in a 130bp product. The fragment of 268bp corresponds to the *B-globin*. The absence of *GSTT1* (in the presence of a *B-globin* PCR product) indicates a *GSTT1* null genotype.

References

1. Li H. Aligning sequence reads, clone sequences and assembly contigs with BWA-MEM. arXiv:13033997 [Epub ahead of print].

2. Saunders CT, Wong WSW, Swamy S, Becq J, Murray LJ, Cheetham RK. Strelka: accurate somatic small-variant calling from sequenced tumor-normal sample pairs. Bioinforma Oxf Engl 2012;28(14):1811–1817.

3. Larson DE, Harris CC, Chen K, et al. SomaticSniper: identification of somatic point mutations in whole genome sequencing data. Bioinformatics 2012;28(3):311–317.

4. Juskevicius D, Ruiz C, Dirnhofer S, Tzankov A. Clinical, morphologic, phenotypic, and genetic evidence of cyclin D1-positive diffuse large B-cell lymphomas with CYCLIN D1 gene rearrangements. Am J Surg Pathol 2014;38(5):719–727.

5. Swerdlow SH, World Health Organization, International Agency for Research on Cancer, editors. WHO classification of tumours of haematopoietic and lymphoid tissues. Revised 4th edition. Lyon: International Agency for Research on Cancer; 2017.

6. Meyer PN, Fu K, Greiner TC, et al. Immunohistochemical methods for predicting cell of origin and survival in patients with diffuse large B-cell lymphoma treated with rituximab. J Clin Oncol Off J Am Soc Clin Oncol 2011;29(2):200–207.

7. Meier C, Hoeller S, Bourgau C, et al. Recurrent numerical aberrations of JAK2 and deregulation of the JAK2-STAT cascade in lymphomas. Mod Pathol Off J U S Can Acad Pathol Inc 2009;22(3):476–487.

8. Novak U, Rinaldi A, Kwee I, et al. The NF-{kappa}B negative regulator TNFAIP3 (A20) is inactivated by somatic mutations and genomic deletions in marginal zone lymphomas. Blood 2009;113(20):4918–4921.

9. Tzankov A, Xu-Monette ZY, Gerhard M, et al. Rearrangements of MYC gene facilitate risk stratification in diffuse large B-cell lymphoma patients treated with rituximab-CHOP. Mod Pathol Off J U S Can Acad Pathol Inc 2014;27(7):958–971.

10. Johnson NA, Slack GW, Savage KJ, et al. Concurrent expression of MYC and BCL2 in diffuse large B-cell lymphoma treated with rituximab plus cyclophosphamide, doxorubicin, vincristine, and prednisone. J Clin Oncol Off J Am Soc Clin Oncol 2012;30(28):3452–3459.

11. Visco C, Li Y, Xu-Monette ZY, et al. Comprehensive gene expression profiling and immunohistochemical studies support application of immunophenotypic algorithm for molecular subtype classification in diffuse large B-cell lymphoma: a report from the International DLBCL Rituximab-CHOP Consortium Program Study. Leukemia 2012;26(9):2103–2113.

12. Hoeller S, Schneider A, Haralambieva E, Dirnhofer S, Tzankov A. FOXP1 protein overexpression is associated with inferior outcome in nodal diffuse large B-cell lymphomas with non-germinal centre phenotype, independent of gains and structural aberrations at 3p14.1. Histopathology 2010;57(1):73–80.

13. Roberti A, Dobay MP, Bisig B, et al. Type II enteropathy-associated T-cell lymphoma features a unique genomic profile with highly recurrent SETD2 alterations. Nat Commun 2016;712602.